

本文参考文献引用格式:杨兆庆,李金梅,梁小武,等. 08Ni3DR 钢焊接接头最薄弱区域与冲击韧性之间的关系[J]. 电焊机, 2021, 51(2):17-23.

08Ni3DR 钢焊接接头最薄弱区域与冲击韧性之间的关系

杨兆庆¹, 李金梅², 梁小武³, 雷万庆², 张建晓³, 曹睿¹, 陈剑虹¹

(1. 兰州理工大学 省部共建有色金属先进加工与再利用国家重点实验室, 甘肃 兰州 730050; 2. 兰州兰石检测技术有限公司, 甘肃 兰州 730000; 3. 兰州兰石重型装备股份有限公司, 甘肃 兰州 730314)

摘要: 低温压力容器 08Ni3DR 钢在极低温度下(-100℃) 具有较好的强韧性匹配, 在实际工程应用中, 保障焊接接头的低温冲击韧性一直是压力容器制造过程中的难题之一。对于实际的焊接接头, 最薄弱区域的确定以及最薄弱区域的影响对焊接接头的表征具有重要的意义。通过将夏比 V 型缺口开在母材、焊缝、热影响区不同位置处, 系统研究了 08Ni3DR 压力容器钢焊接接头的组织和韧性。结果表明: 焊接接头韧性最薄弱区域为粗晶热影响区, 其粗晶热影响区的显微组织为粗大的粒状贝氏体和板条贝氏体组成的复合组织。粗晶热影响区宽度在缺口尖端前沿所占比例越高, 试样的冲击吸收能量越低。当粗晶热影响区宽度所占比例达到 100% 时, 冲击吸收能量为 27 J, 相比于母材冲击韧性损失高达 90.7%。以上两个方面充分体现出焊接接头最薄弱区域对冲击韧性有很大的影响。

关键词: 08Ni3DR; 最薄弱区域; 粗晶热影响区; 冲击韧性

中图分类号: TG457

文献标志码: A

文章编号: 1001-2003(2021)02-0017-07

DOI: 10.7512/j.issn.1001-2303.2021.02.03

0 前言

近几十年来随着石油、化工产品的消费迅速上升, 尤其是乙烯工业的飞速发展, 对低温及超低温用结构材料的需求越来越大, 低温材料作为重要的战略物资, 国内各大钢厂都在进行研究, 这就对大型低温装置的建设提出了更高的要求^[1-3]。低温压力容器 08Ni3DR 钢在极低温度下(-100℃) 具有较好的强韧性匹配, 已被广泛用于存储包括乙烯、低温甲醇洗、城市燃气、二氧化碳等低温装置中。在实际的工程应用中, 熔焊技术是制造大型压力容器结构必不可少的技术。但是, 保障焊接接头的低温冲击韧性一直是压力容器制造过程中的难题之一。焊接

接头热影响区(heat affected zone, HAZ)中的粗晶热影响区(coarse grain heat affected zone, CGHAZ)有可能产生粗大晶粒和损害韧性的微观组织, 例如粒状贝氏体、上贝氏体、马氏体、侧板条铁素体等^[4-6], 从而成为诱发解理裂纹失稳扩展, 引发断裂的最薄弱区域^[7-8]。因此这不仅需要提高压力容器设备的冲击性能, 而且还必须具有优良的可焊接性^[9]。目前, 国内外学者大多采用热模拟技术或通过改变焊接参数来研究热影响区的性能, 其结果仅能反映焊接接头在一定热模拟参数下的力学性能, 并不能反映钢材的真实可焊性及其对焊接的适应性。实际焊接接头中的热影响区是一个很窄的区域, 最薄弱的粗晶热

收稿日期: 2020-11-17

基金项目: 国家自然科学基金项目(51761027, 51675255); 兰州市科技计划项目(2019-1-49)

作者简介: 杨兆庆(1995—), 男, 硕士, 主要从事焊接热影响区韧性的研究。E-mail: 541110209@qq.com。

通讯作者: 曹睿(1977—), 女, 教授, 博导。E-mail: caorui@lut.edu.cn。

影响区是一个狭小的微区,单独表征实际焊接接头中热影响区的冲击韧性是非常困难的,并且热影响区特别是粗晶热影响区占缺口尖端 8 mm 韧带不同比例时冲击韧性是不一样的。因此通过将缺口尖端开在焊接接头热影响区不同位置处,通过一系列实验得出不同比例的粗晶热影响区试样所对应的冲击韧性以及焊接接头最低的冲击韧性,综合以上两个方面来体现焊接接头最薄弱区域对冲击韧性的影响。基于此,文中揭示了 08Ni3DR 焊条电弧焊焊接接头的最薄弱区域,结合热影响区的组织、硬度、断口形貌,从理论上研究了缺口位于热影响区不同位置时最薄弱区域在缺口试样 8 mm 韧带上占的比例与冲击韧性之间的关系。为承压设备常用材料焊接接头最薄弱区域韧性的合格指标提供数据支撑,为建立钢材焊接最薄弱区域对冲击韧性的评价方法提供理论基础。

1 实验材料与方法

实验母材采用 08Ni3DR 压力容器低温钢板,厚度 32 mm,母材化学成分如表 1 所示。焊前预热温度为 120~160 °C,焊后热处理工艺为 590 °C,保温 4 h,开 V 型坡口。焊条电弧焊采用 OERLIKON 公司生产的 E7016-C2L 焊条,其熔敷金属化学成分如表 2 所示。焊接工艺参数为:热输入 15 kJ/cm,焊接电流 150~160 A,焊接电压 30 V,焊接速度 10 m/h。在板厚的 1/4 处取横向试样,缺口方向垂直于焊接方向。试样参照并执行国家标准 GB/T 2650-2008《焊接接头冲击试验方法》进行取样加工,标准的夏比 V 型缺口分别取在母材 (base metal, BM),焊缝 (weld metal, WM) 和热影响区。将热影响区划分为粗晶热影响区 (CGHAZ),细晶热影响区 (fine grained heat affected zone, FGHAZ),临界热影响区 (intercritical heat affected zone, ICHAZ),亚临界热影响区 (subcritical heat affected zone, SCHAZ)。选取熔合线较为平直的试样,将缺口取在熔合线处 (粗晶热影响区),如图 1 所示。细晶热影响区缺口开在距离熔合线 1 mm 处,临界热影响区缺口开在距离熔合线 1.5 mm 处,亚临界热影响区缺口开在距离熔合线 2 mm 处。通过带有千分尺的光学显微镜在左右移动距离为 0.1 mm 的范围内统计出缺口尖端粗晶热影响区宽度所占 8 mm 缺口尖端前沿的比例。使用 CIEM-300-CPC 电气测量冲击试验机在 -100 °C 下进行低温冲击试验。

其中,母材、焊缝各制备 5 个冲击试样,粗晶热影响区制备 50 个冲击试样,热影响区其他区域制备 10 个冲击试样。采用 Quanta450FEG 型扫描电子显微镜 (SEM) 分析组织和断口形貌。采用 HAT-1000A 数字显示显微硬度仪测量显微硬度。

表 1 08Ni3DR 钢化学成分

Table 1 Composition of 08Ni3DR steel %

w(C)	w(Mn)	w(Si)	w(S)	w(P)
0.08	0.68	0.22	0.002	0.002
w(Ni)	w(Mo)	w(V)	w(Al)	
3.55	0.070	0.01	0.017	

表 2 E7016-C2L 焊条熔敷金属化学成分

Table 2 Chemical composition of E7016-C2L electrode deposited metal %

w(C)	w(Mn)	w(Si)	w(S)	w(P)	w(Cr)
0.027	0.620	0.187	0.005	0.010	0.020
w(Mo)	w(Ni)	w(Nb)	w(Cu)	w(V)	
0.006	3.640	0.002	0.014	0.002	

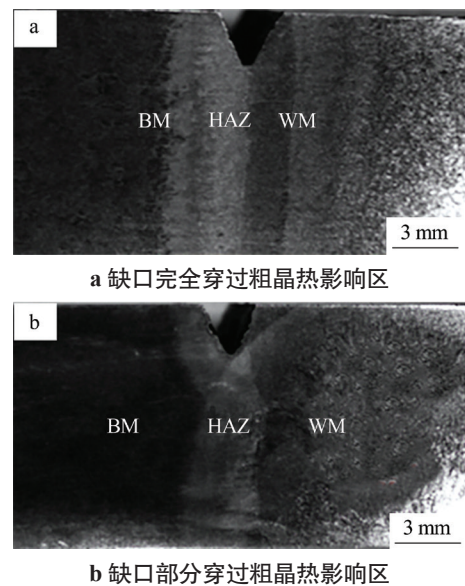


图 1 焊接接头热影响区冲击试样缺口位置

Fig.1 Location of the notch of the impact specimen in the HAZ of the welded joint

2 结果与分析

2.1 焊接接头各区域的冲击吸收能量

08Ni3DR 钢焊接接头在 -100 °C 下各区域的冲击吸收能量如表 3 所示。-100 °C 时,母材、亚临界热影响区、临界热影响区、细晶热影响区的平均冲

击吸收能量均在 270 J 以上,都具有优异的冲击韧性,焊缝的平均冲击吸收能量为 158 J,冲击韧性表现良好。通过一系列实验得到缺口尖端冲击试样前沿含有粗晶热影响区的冲击吸收能量最低只有 41 J,粗晶热影响区的冲击吸收能量相比焊接接头其他区域差异巨大,其冲击吸收能量相比于母材损失了约 86%,成为韧性最薄弱的区域。08Ni3DR 钢焊接接头各区域在 -100 °C 下的冲击断口形貌如图 2 所示。母材、亚临界热影响区、临界热影响区、细晶热影响区的断口都被韧性断裂区覆盖,在微观断口上展现出河流状花样的解理台阶、韧窝、撕裂脊共存的现象,表现为准解理断裂。

表 3 08Ni3DR 焊接接头 -100 °C 下各区域的平均冲击吸收能量

Table 3 Impact absorbed energy of each zone for 08Ni3DR welded joints at -100 °C

BM	SCHAZ	ICHAZ	FGHAZ	不同比例的 CGHAZ 焊接接头	WM
290	282	272	291	41~305	158

韧性断裂。焊缝金属的断口由解理区和韧性断裂区共同组成,在微观断口上展现出河流状花样的解理台阶、韧窝、撕裂脊共存的现象,表现为准解理断裂。

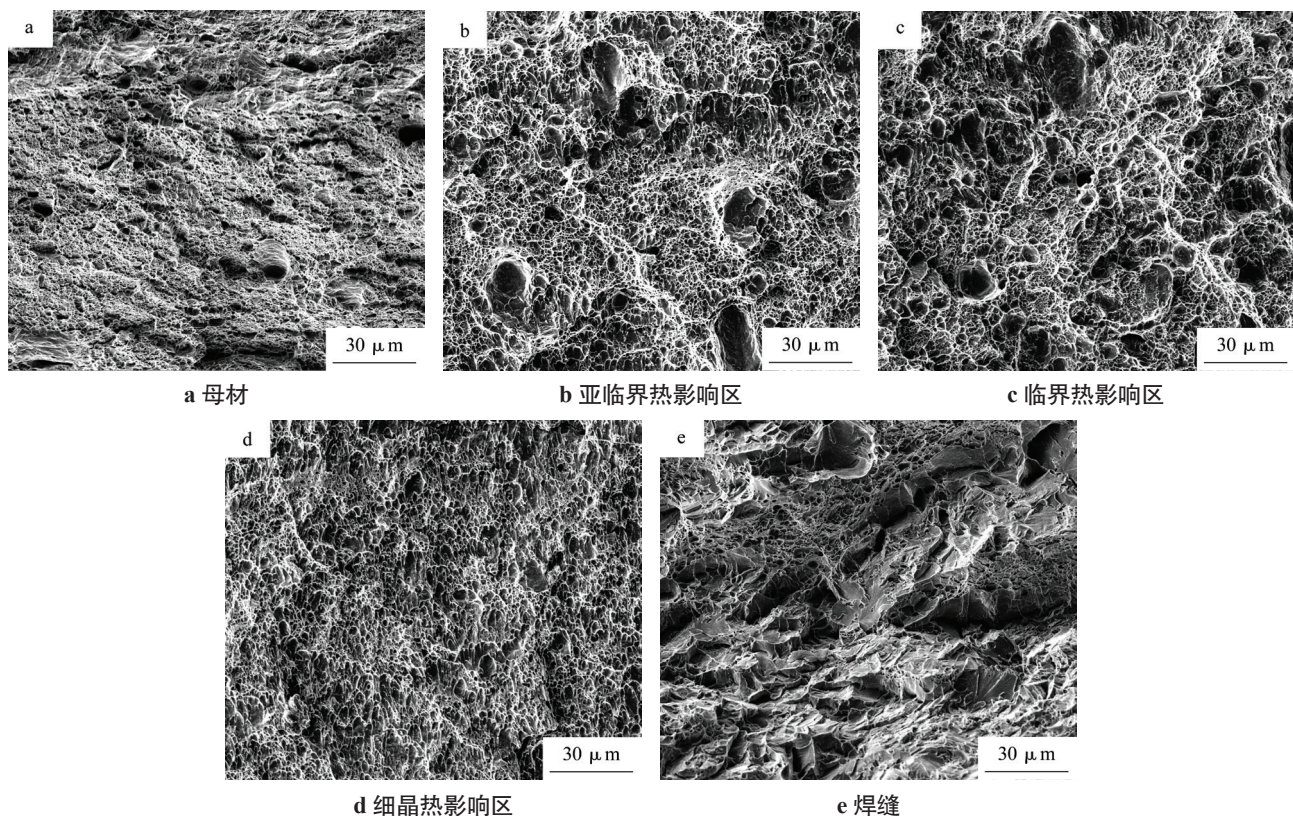


图 2 焊接接头冲击断口形貌

Fig.2 Impact fracture surfaces of in various regions of the welded joint

2.2 焊接接头各区域的微观组织及硬度

08Ni3DR 钢焊接接头各区域的显微组织如图 3 所示。亚临界热影响区组织与母材相比,均为块状铁素体,且基体上弥散分布有少许碳化物。临界热影响区组织为晶粒尺寸差异较大的铁素体,这可能是由于一部分组织发生奥氏体化,在冷却的过程中转变为细小的晶粒,其余部分仍保持原来晶粒较大的尺寸。因此,此区域的组织由一部分未转变的较粗大晶粒和已转变的细小晶粒组成。细晶热影

响区的组织由晶粒尺寸均一且细小的块状铁素体(Block ferrite, BF)组成。粗晶热影响区组织发生严重的粗化,在冷却过程中,产生粒状贝氏体(Granular ferrite, GB)和板条贝氏体(Lath bainite, LB)组成的复合组织。焊缝一次组织为粗大的柱状晶,分布有少量碳化物,在晶界内形成细小的针状铁素体(Acicular ferrite, AF)。二次组织为块状铁素体,且尺寸较为均匀。晶粒尺寸分布如图 4 所示。由图可知,母材的平均晶粒尺寸为 13.5 μm,最大为 27 μm;亚临

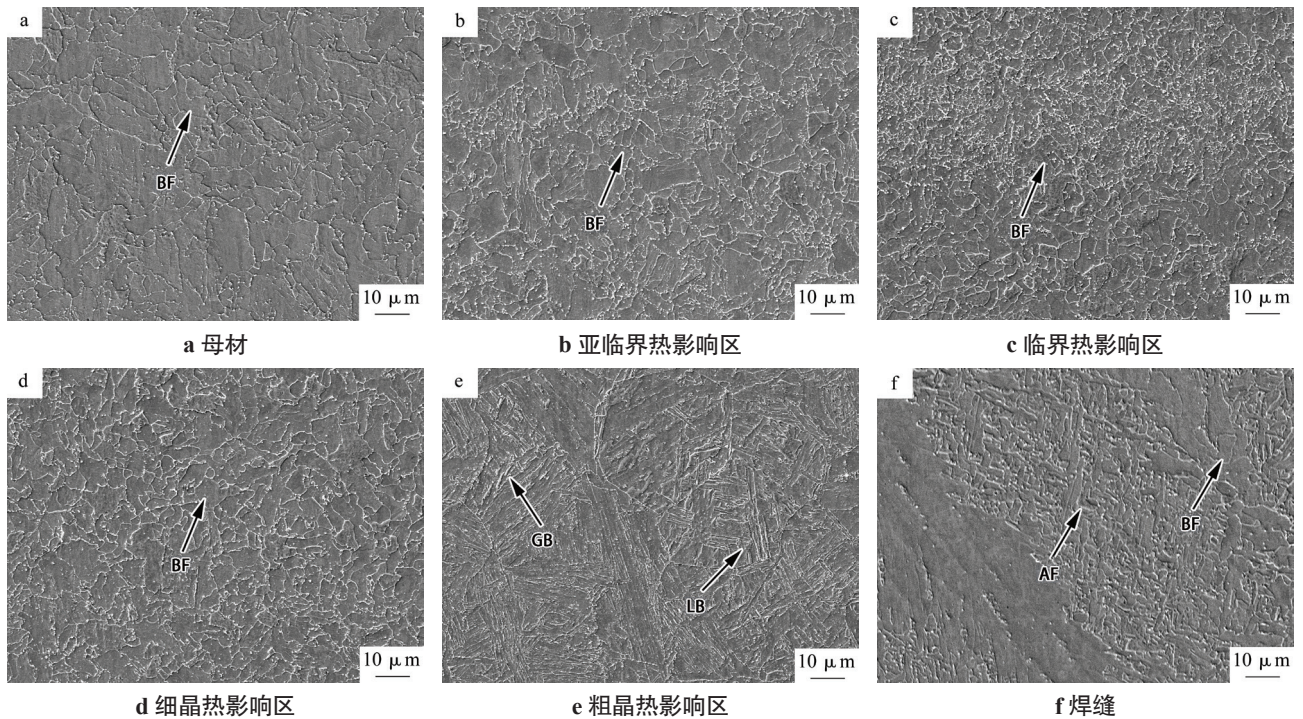


图3 08Ni3DR 焊接接头各区域的显微组织

Fig.3 Microstructures in various regions of the welded joint

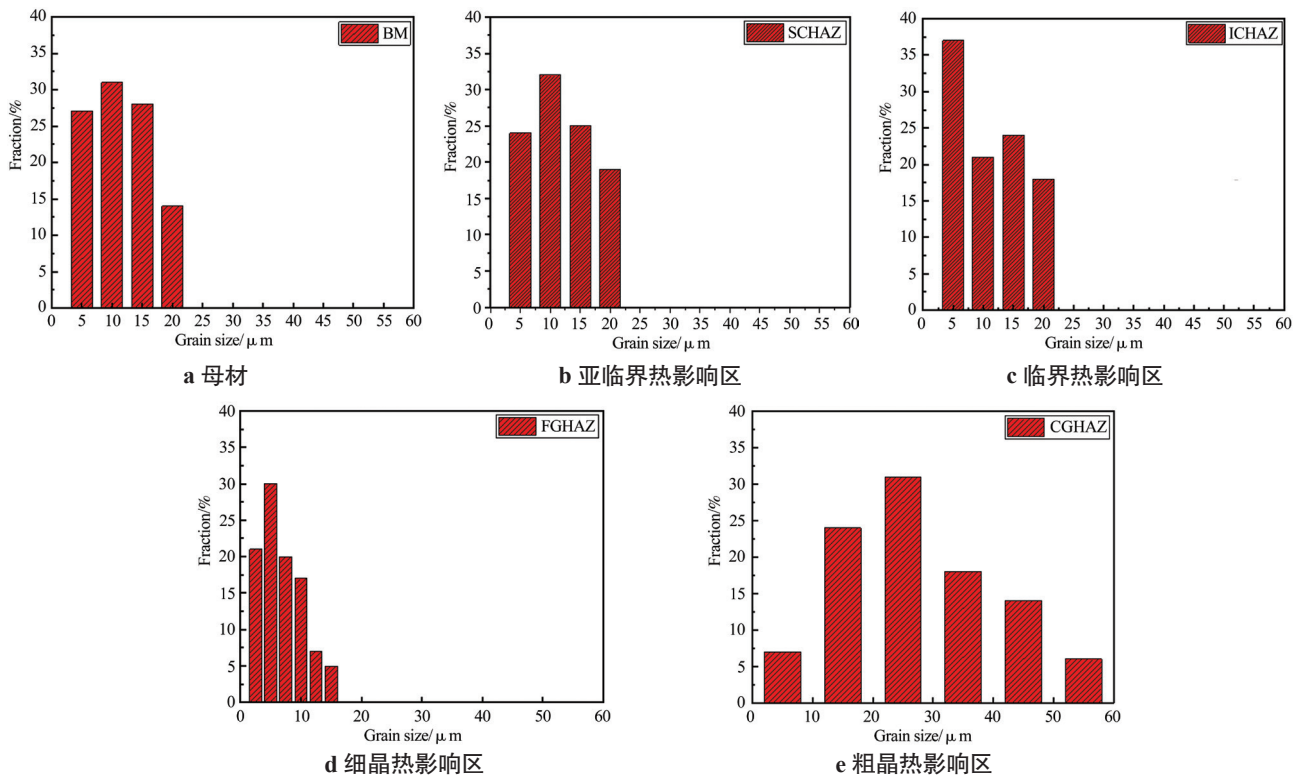


图4 焊接接头晶粒尺寸分布

Fig.4 Distribution of grain size of the welded joint

界热影响区的平均晶粒尺寸为 $13.7 \mu\text{m}$, 最大为 $27 \mu\text{m}$; 临界热影响区的平均晶粒尺寸为 $11.5 \mu\text{m}$,

最大为 $26 \mu\text{m}$; 细晶热影响区的平均晶粒尺寸为 $7.8 \mu\text{m}$, 最大为 $18 \mu\text{m}$; 而粗晶热影响区的平均晶

粒尺寸为 25 μm , 最大为 55 μm 。通过比较图 3 的微观组织以及图 4 的晶粒尺寸分布可知, 母材、细晶热影响区、粗晶热影响区的晶粒尺寸差异较大。虽然临界热影响区的晶粒尺寸不均匀, 但平均晶粒尺寸和母材、亚临界热影响区的晶粒尺寸相近。相比细晶热影响区, 粗晶热影响区的晶粒尺寸粗化显著。焊缝、热影响区以及母材的硬度分布如图 5 所示。远离熔合线的亚临界热影响区平均硬度最小, 显微硬度值为 157~164 HV, 相对于母材硬度值的 168~181 HV 发生少许软化。临界热影响区和细晶热影响区相比母材, 硬度有所提升。紧邻熔合线的焊缝和粗晶热影响区的硬度较高, 而粗晶热影响区表现出最高的硬度, 硬度平均值达到 210~231 HV。

2.3 粗晶热影响区宽度占缺口尖端前沿比例与冲击吸收能量的关系

通过一系列缺口试样的研究, 将缺口开在熔合线处, 发现冲击吸收能量在 41~305 J 范围内波动, 说明缺口尖端前沿粗晶热影响区组织比例的不同, 会严重影响缺口试样的冲击韧性。缺口尖端开在熔合线处, 但韧带上含有不同比例不同区域的混合组织, 断口形貌如图 6 所示。比较图 6 可知, 缺口尖端呈现准解理断裂区域的不同, 最后决定了不同试样存在不同的冲击韧性, 而且随着呈现准解理断裂区域的粗晶热影响区比例的增加, 冲击韧性随之降低。通过测量缺口尖端粗晶热影响区宽度分布比例, 得

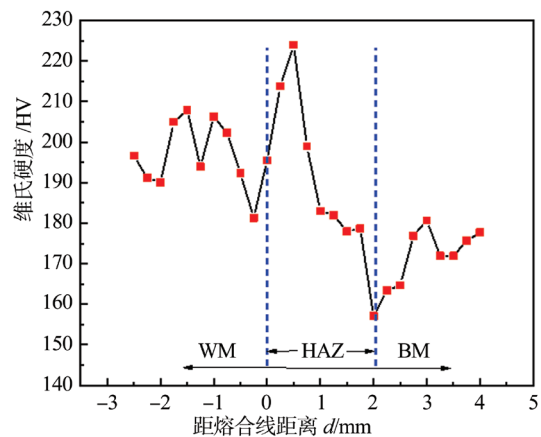


图 5 08Ni3DR 钢焊接接头的硬度分布曲线

Fig.1 Vickers hardness distribution of 08Ni3DR steel welded joint

到不同粗晶热影响区宽度的断口形貌。当冲击吸收能量在 270 J 以上时, 缺口尖端并没有粗晶热影响区组织的存在, 因而对其韧性并没有削弱。当冲击吸收能量下降到 233 J 时, 测得粗晶热影响区宽度所占比例达到整个韧带区的 21.7%, 断口由大量的韧性断裂区和 21.7% 的脆性解理断裂区组成。当冲击吸收能量下降到 123 J 时, 粗晶热影响区宽度所占比例达到了 62.1%, 断口由少量的韧性断裂区和 62.1% 的脆性解理断裂区组成。当冲击吸收能量降低到 47 J 时, 粗晶热影响区宽度所占比例达到了 86.5%, 断口上大部分由脆性解理断裂区组成, 仅有少许韧性断裂区, 此时, 相比于母材冲击吸收能

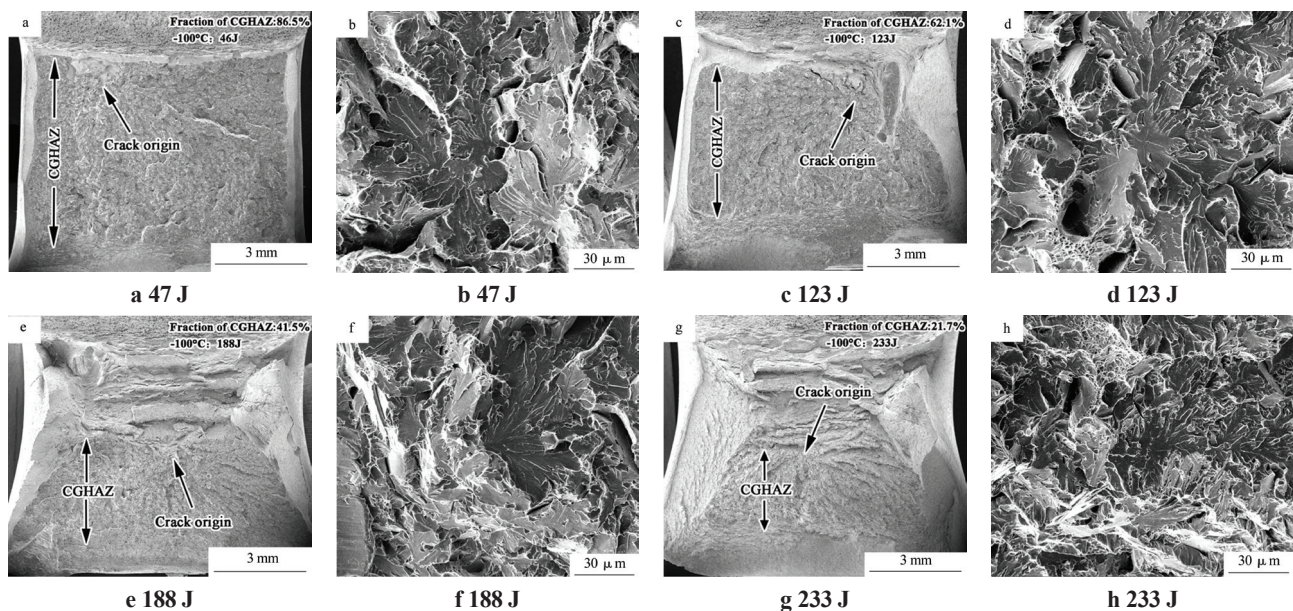


图 6 缺口前沿占有不同比例粗晶热影响区的冲击试样断口的宏观形貌

Fig.6 Fracture surface morphologies of CGHAZ of different fractions

量损失了约 86%。虽然在实际施焊条件下,并没有出现粗晶热影响区宽度所占百分比例的缺口试样,但是可以通过粗晶热影响区的分布比例与冲击韧性的分布曲线(见图 7),通过函数拟合公式,从而间接地计算出 100% 粗晶热影响区宽度所占比例相对应的冲击韧性。完整的粗晶热影响区的冲击吸收能量拟合值为 27 J(非实验线性拟合值)。从曲线分布来看,总体趋势为:随着粗晶热影响区所占缺口尖端前沿的比例增加冲击韧性逐渐降低。

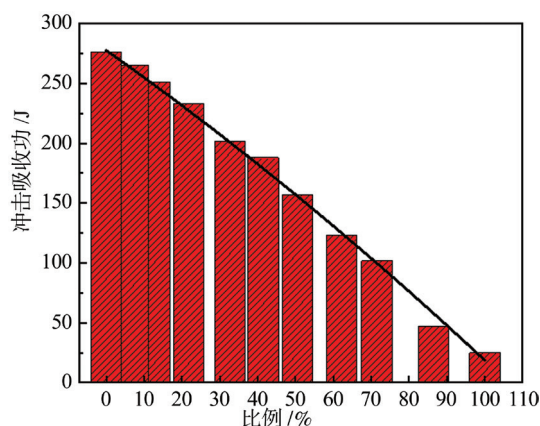


图 7 08Ni3DR 钢缺口尖端前沿粗晶热影响区的分布比例与冲击韧性

Fig.7 Fraction of CGHAZ in front of the notch tip and impact toughness of 08Ni3DR steel

2.4 焊接接头最薄弱区域的确定

焊接接头热影响区中的局部脆性大多是由粗晶热影响区引起的。由于晶粒的显著粗化,这使得热影响区和母材的性能严重失配。粗晶热影响区的显微组织通常是粒状贝氏体、多边形铁素体和M-A 组元组成的混合显微组织,区别主要在于贝氏体、铁素体的晶粒尺寸以及M-A 组元的尺寸和含量^[10-13]。在本研究中,母材、细晶热影响区、粗晶热影响区的平均晶粒尺寸分别为 13.5 μm、7.8 μm、25 μm,最大平均晶粒尺寸为 27 μm、18 μm、55 μm。细晶热影响区的平均晶粒尺寸约为粗晶热影响区晶粒尺寸的 1/3。结合焊接接头各区域的硬度值,临界热影响区与细晶热影响区的硬度相比母材有所提升,其原因可能是晶粒细化所导致的细晶强化。同时,粗晶热影响区的组织为粒状贝氏体和板条贝氏体组成。而其他区域为单一的铁素体组成。因此,韧性的提高是由更细小的单一晶粒组织引起的。粗晶热影响区和细晶热影响区之间冲击韧性的主要差异是晶粒尺寸和组织不同所致^[14-15]。对比各个区域的显微

组织,由于粗晶热影响区有贝氏体出现,而其他区域并不存在,因而表现出更高的硬度(210~231 HV),大于焊接接头任何区域的硬度。所以,显微组织由粗大的粒状贝氏体以及板条贝氏体组成的粗晶热影响区表现出最差的冲击韧性,而晶粒尺寸较细小且组织组成较单一的母材、亚临界影响区、临界热影响区、细晶热影响区拥有更好的冲击韧性。上述实验结果表明,08Ni3DR 钢焊接接头的最薄弱区域是粗晶热影响区,而粗大的粒状贝氏体+板条贝氏体是韧性最弱的显微组织,这是粗晶热影响区韧性差的最直接原因。

2.5 最薄弱区域比例对冲击韧性的影响规律

由于缺口位置的差异,冲击吸收能量的差异超过了 250 J 左右。粗晶热影响区的宽度随热影响区熔合线中缺口位置的微小变化而发生显著变化。随着缺口尖端的粗晶热影响区分数的增加,冲击吸收能量逐渐降低,直到达到 27 J(非实验线性拟合值),这表明缺口尖端的微观组织对冲击韧性有很大的影响。与母材和热影响区其他区域的韧性相比,最薄弱的粗晶热影响区的冲击韧性降低了约 90.7%。因此,也进一步说明最薄弱区域在缺口尖端前的分布位置和所占比例对整体焊接接头冲击韧性有很大的影响。当缺口尖端前沿没有粗晶热影响区时,冲击吸收能量大于 270 J,缺口尖端前沿的组织由韧性较好的细晶热影响区所组成,试样为完全的韧性断裂。因此,08Ni3DR 焊接接头试样中冲击吸收能量从 41 J 变化到 305 J,断裂模式从解理断裂—准解理断裂—韧性断裂逐渐转变,其中主要的原因是在缺口尖端韧带上存在一定比例的粗晶热影响区。这表明除了粗晶热影响区外,其他区域的组织在实验温度下表现出更好的韧性。如果在实际焊接条件下无法获得完整粗晶热影响区的冲击韧性,根据图 7 可以通过函数模型拟合公式计算出完整的粗晶热影响区所对应的冲击韧性。基于上述讨论,焊接接头缺口试样冲击韧性的差异主要来自于缺口尖端前沿最薄弱区域的分布位置和比例。而最薄弱区域的组织组成决定了该区域的强韧性,因而最薄弱区域在缺口尖端前沿的比例也就影响着缺口试样的冲击韧性。

3 结论

(1) 08Ni3DR 钢焊条电弧焊焊接接头在热输入为 15 kJ/cm 的情况下,最薄弱区域为粗晶热影响区,微

观组织由粗大的粒状贝氏体以及板条贝氏体组成,其冲击吸收能量为 27 J(非实验线性拟合值)。相对于母材冲击吸收能量降低约 90.7%。粗晶热影响区韧性恶化的根本因素是微观组织的转变以及晶粒的粗化。

(2)在实际焊接接头中,最薄弱区域在缺口尖端前沿所占的比例越多,相对应的冲击韧性越低。最薄弱区域占缺口尖端前沿韧带 60%~70% 时,冲击吸收能量相比母材损失了约 70%。当最薄弱区域占缺口尖端前沿的 90%~100% 时,冲击吸收能量相比母材损失了约 90%,充分展现出焊接接头最薄弱区域对缺口试样的冲击韧性有巨大影响。如果在实际施焊条件下,没有得到完整的最薄弱区域的冲击韧性,可以通过拟合的函数模型,从而间接计算出最薄弱区域宽度所占比例相对应的冲击韧性。

参考文献:

- [1] 张勇. 低温压力容器用钢的现状与发展概况[J]. 压力容器, 2006, 23(4):31-34.
- [2] 徐亮,章小浒,黄金国,等. 首台-100 °C用 08Ni3DR 钢制 3 000 m³ 乙烷球罐的制造焊接工艺[J]. 电焊机, 2017, 47(5):137-143.
- [3] 李道清,高小红,任世宏,等. 3.5Ni 低温钢的焊接[J]. 电焊机, 2012, 42(10):52-57.
- [4] Lan L Y, Qiu C L, Zhao D W, *et al.* Microstructural characteristics and toughness of the simulated coarse grained heat affected zone of high strength low carbon bainitic steel[J]. Materials Science and Engineering A, 2011, 529(11): 192-200.
- [5] 张英乔,张汉谦,刘伟明. M-A 组元对石油储罐用钢粗晶热影响区韧性的影响[J]. 焊接学报, 2009, 30(1): 112-115.
- [6] Yang Y, Cheng J S, Nie W J, *et al.* Investigation on the microstructure and toughness of coarse grained heat affected zone in X-100 multi-phase pipeline steel with high Nb content[J]. Materials Science and Engineering A, 2012, 558(12):692-701.
- [7] 秦华,苏允海,连景宝. BWELDY960Q 钢焊接热模拟热影响区组织与性能[J]. 焊接学报, 2018, 39(11):97-101.
- [8] 白世武,李午申,邸新杰,等. 07MnNiCrMoVDR 钢焊接粗晶热影响区的韧化机理[J]. 焊接学报, 2008, 29(3): 25-28.
- [9] Xie H, Du L X, hu J, *et al.* Microstructure and mechanical properties of a novel 1000 MPa grade TMCP low carbon microalloyed steel with combination of high strength and excellent toughness[J].Materials Science and Engineering A, 2014, 612(8):123-130.
- [10] 文明月,董文超,庞辉勇,等. 一种 Fe-Cr-Ni-Mo 高强钢焊接热影响区的显微组织与冲击韧性研究[J]. 金属学报, 2018, 54(4):501-511.
- [11] 崔冰,彭云,彭梦都,等. 热循环对 Q890 钢焊接热影响不同区域组织及性能的影响[J]. 焊接学报, 2017, 38(7): 35-39.
- [12] Zhou Y L, Jia T, Zhang X J, *et al.* Microstructure and toughness of the CGHAZ of an offshore platform steel[J]. Journal of Materials Processing Technology, 2015, 219(5): 314-320.
- [13] 陈延清,杜则裕,许良红. X80 管线钢焊接热影响区组织和性能分析[J]. 焊接学报, 2010, 31(5):18-22.
- [14] Cao R, Yang Z Q, Chan Z S, *et al.* The determination of the weakest zone and the effects of the weakest zone on the impact toughness of the 12Cr2Mo1R welded joint[J]. Journal of Manufacturing Processes, 2020, 50(2):539-546.
- [15] Yang S, Ju L, Cong W. On the heterogeneous microstructure development in the welded joint of 12MnNiVR pressure vessel steel subjected to high heat input electrogas welding[J].Journal of Materials Science & Technology, 2019, 35(8):1747-1752.

MAIN TOPICS, ABSTRACTS & KEY WORDS

Research development of composite green brazing materials of filler metal and flux

WANG Bo¹, LONG Weimin^{1,2}, ZHONG Sujuan², XUE Songbai³, GUAN Shaokang⁴, CHENG Yafang²

(1.China Innovation Academy of Intelligent Equipment Co., Ltd., Ningbo 315700, China; 2.State Key Laboratory of Advanced Brazing Filler Metals and Technology, Zhengzhou Research Institute of Mechanical Engineering Co., Ltd., Zhengzhou 450001, China; 3.College of Material Science and Technology, Nanjing University of Aeronautics and Astronautics, Nanjing 211106, China; 4.Henan Key Laboratory of Advanced Magnesium Alloy, Zhengzhou University, Zhengzhou 450002, China). pp 1–9

Abstract: Brazing is one of the key basic technologies in the manufacturing industry, and the wide application of composite brazing filler metals is an important method to realize green and automatic brazing. Comparing with the traditional filler metal, composite filler metal can achieve the precise flux reaction under the conditions of accurate positioning, constant temperature, timing and quantification. In this article, the classification and characteristics of brazing filler metals at home and abroad are reviewed, and the preparation technology, composition design and typical applications of flux-cored brazing filler metals, flux-coated brazing filler metals, brazing filler metals prepared by powder are analyzed. The shortcomings of current research are pointed out, and suggestions for the future development of the composite filler metal are put forward. For example, with the aid of materials genome technology, developing low-Ag and Cd-free brazing filler metal with high activity and low emissions; continuously innovating the processing and preparation technology of composite brazing filler metals, such as friction stir processing and electromagnetic plastic technology; developing continuous plate-packed and barrel-packed flux-cored composite brazing filler metals with excellent surface quality to replace traditional manual strip brazing filler metals.

Key words: composite brazing filler metal; flux-cored brazing filler metal; flux-coated brazing filler metal; brazing filler metal prepared by powder

Friction stir welding of aluminum alloy heat source model expert system

LIU An¹, HU Guangxu¹, DONG Zhibo²

(1.Department of Mechanical, Harbin University of Commerce, Harbin 150028, China; 2.State Key Laboratory of Advanced Welding and Joining, Harbin Institute of Technology, Harbin 150001, China). pp 10–16

Abstract: In establishing model process of three-dimensional heat source model of aluminum alloy friction stir welding, heat flux density range of shoulder, stir pin's side and bottom generating heat quantity is uncertain, which needs certainty through verification, increases the difficulty and workload of modeling. For this problem, three-dimensional friction stir weld heat source model is established, and uncertain parameters in heat source model are determined. At the same time, effect of these parameters changing for welding temperature is researched in the simulation. In addition, according to the effect law of parameters changing, library of parameters of friction stir welding heat source is established and inference rules are designed. Friction stir welding of aluminum alloy heat source model expert system of fast establishing model are achieved. Finally, temperature field results of friction stir welding experiment have validated expert system function. Expert system significantly reduce difficulty of numerical simulation of friction stir welding, and is beneficial to promote the popularization and application of numerical simulation technology of friction stir welding of aluminum alloy.

Key words: friction stir welding; aluminum alloy; heat quantity; heat flux density; expert system

Relationship between the weakest zone and impact toughness of 08Ni3DR welded joint

YANG Zhaoqing¹, LI Jinmei², LIANG Xiaowu³, LEI Wanqing², ZHANG Jianxiao³, CAO Rui¹, CHEN Jianhong¹

(1.State Key Laboratory of Advanced Processing and Recycling of Nonferrous Metals, School of Materials Science and Engineering, Lanzhou University of Technology, Lanzhou 730050, China; 2.Lanzhou Ls Testing Technology Co., Ltd., Lanzhou 730000, China; 3.Lanzhou Ls Heavy Equipment Co., Ltd., Lanzhou 730314, China). pp 17–23

Abstract: Low temperature pressure vessel 08Ni3DR steel has a good strength and toughness at a very low temperature (–100 °C). In practical engineering application, it is one of the difficult problems to ensure the low temperature impact toughness of welded joints in the process of pressure vessel manufacturing. The determination of the weakest zone and the effects of the weakest zone are very important for the charac-

erization of the actual welded joints. The microstructures and toughness of the welded joints of 08Ni3DR pressure vessel steel were systematically studied by preparing the Charpy V-notch on the base metal, weld metal and different locations of heat-affected zone. The results show that the weakest toughness zone of the welded joint is the coarse grain heat-affected zone, which is a composite microstructure composed of coarse granular bainite and lath bainite. As the proportion of the width of coarse grain heat affected zone in the front of the notch tip increases, the impact absorbed energy of the specimen decreases. When the proportion of the width of the coarse grain heat-affected zone reaches 100%, the impact absorbed energy is 27 J, and the impact toughness of the coarse grain heat-affected zone reduces by 90.7%. Above two aspects fully show that the weakest zone has a great effect on the impact toughness of the welded joint.

Key words: 08Ni3DR steel; the weakest zone; coarse grain heat affected zone; impact toughness

Effect of rotation speed on the microstructure and mechanical properties of friction stir welded joints of 6061 aluminum alloy and pure copper dissimilar metals

QIN Jiachen^{1,2}, ZHANG Datong¹, TAN Jinhong², YOU Jiaqing², ZHAO Yunqiang²

(1. National Engineering Research Center of Near-Net-Shape Forming for Metallic Materials, School of Mechanical and Automotive Engineering, South China University of Technology, Guangzhou 510640, China; 2. China-Ukraine Institute of Welding, Guangdong Academy of Sciences, Guangzhou 510651, China). pp 24-30

Abstract: In this paper, 6061-T6 aluminum alloy and pure copper are welded by friction stir welding and the effect of rotation speed on the microstructure and mechanical properties of dissimilar joints is studied. When the welding speed is 30 mm/min and the rotation speed is in the range of 1 200 r/min to 1 800 r/min, sound joints without defects can be obtained. The complex structures are formed in the nugget zone where a large number of broken Cu particles are stirred into. Al₂Cu, Al₄Cu₉ and AlCu intermetallic compounds are found in the nugget zone. The intermetallic compound layer is formed by mutual diffusion between aluminum and copper at the interface. With the increase of rotation speed, the compounds layer gradually becomes thicker. Due to the grain refinement, solid solution strengthening and the appearance of the IMCs, the average microhardness of the nugget zone is higher than that of aluminum and copper sides, and the microhardness peak appears in the nugget zone. Meanwhile, the tensile strength of the joint firstly increases and

then decreases. The tensile strength of the optimal joint is 183 MPa and the joint efficiency is up to 71.8% of Cu BM. The fracture occurs in the heat affected zone of Al side, and the fracture mode is a ductile fracture.

Key words: 6061 aluminum alloy; pure copper; friction stir welding; microstructure; mechanical properties

Finite element analysis of welding temperature field and stress field of S355 steel

DUAN Weijun¹, DENG Hongjian¹, CHEN Beiping¹, QIU Peixian¹, CHEN Jingqing² (1. CRRC Qingdao Sifang Rolling Stock Co., Ltd, Qingdao 266311, China; 2. Southwest JiaoTong University, Chengdu 610031, China). pp 31-36

Abstract: S355 steel is a low alloy steel, which is accompanied by solid phase transformation during welding. Based on the solid phase transformation effect of S355 steel, a thermal-stress finite element model of welding process was established. The microstructure evolution law in the weld and heat affected zone was analyzed. The results show that under the effect of solid phase transformation, the Mises stress of the weld decreased. The residual stress and deformation evolution curves of the heat affected zone with and without phase transformation were compared. The calculated residual stress was in good agreement with the measured value.

Key words: S355 steel; solid state transformation; microstructure; residual stress

Effect of welding heat input on microstructure and properties of CGHAZ of ultra-low carbon bainitic steel

XU Chunhua¹, XIE Shuxian¹, WANG Hairui², ZHANG Yuxing², FENG Xueyan², LIU Peng²

(1. Shandong CRRC Tongli Steel Structure Co., Ltd., Ji'nan 250101, China; 2. School of Materials Science and Engineering, Shandong Jianzhu University, Ji'nan 250101, China). pp 37-40, 51

Abstract: In order to explore the effect of different welding inputs on the microstructure and impact properties of coarse grain heat-affected zone (CGHAZ) of ultra-low carbon bainitic steel welded joint, Gleeble-3500 thermal simulation machine was used to simulate different inputs to study the effects of different heat inputs on the microstructure and impact toughness of CGHAZ of Q420qEN steel joint. And the CGHAZ was characterized. The results show that as the welding heat input increases, the microstructure of CGHAZ becomes coarser, the lath bainite decreases and granular bainite increases; meanwhile, when the welding heat input increases from 18kJ/cm to 30 kJ/cm, the impact toughness of CGHAZ at -20°C increases first and then decreases.